applied sciences

MDPI

Article

Evaluation of Link Overstrength Factor for the Seismic Design of Eccentrically Braced Frames

Yoonsu Hong and Eunjong Yu *

Department of Architectural Engineering, Hanyang University, Seoul 04763, Republic of Korea; clark1214@hanyang.ac.kr
* Correspondence: eunjongyu@hanyang.ac.kr; Tel.: +82-2-2220-4311

Abstract: In eccentrically braced frames (EBFs), inelastic behavior is only permitted in the links. All members, except for the links, are designed according to the capacity design concept by using the link overstrength factor, Ω, so that they remain elastic even when the links develop their ultimate strength (including the strain-hardening effect). AISC 341 specifies that the Ω factor of link members must be 1.25 for beam and brace design and 1.1 for column design. In this study, the relevance of the current Ω factor was investigated. A total of 471 K-braced EBF systems with various conditions were designed using a multi-objective optimization technique, and nonlinear dynamic analyses were performed to evaluate the Ω factor. The results indicate that it is reasonable to use the current Ω factor for the design of beam outside link and brace; however, it leads to an overestimation of axial force in columns, especially in the lower stories of tall buildings. From the analysis results, a new Ω factor equation for column design was proposed. It was demonstrated that the structural quantities of 15-story frames designed using the proposed equation decreased by an average of 19% compared to those designed using the current Ω factor.

Keywords: eccentrically braced frame; capacity design; multi-objective optimization; link overstrength factor; strain hardening; nonlinear dynamic analysis

Citation: Hong, Y.; Yu, E. Evaluation of Link Overstrength Factor for the Seismic Design of Eccentrically Braced Frames. *Appl. Sci.* **2024**, *14*, 9683. https://doi.org/10.3390/app14219683

Academic Editor: Cesare Biserni

Received: 12 September 2024
Revised: 10 October 2024
Accepted: 17 October 2024
Published: 23 October 2024

1. Introduction

Eccentrically braced frames (EBFs) are lateral-force-resisting systems in which two braces are connected to a beam with an offset. The short segment of the beam between the connection points and braces, which is referred to as the link, is subjected to significant shear forces and moments. In EBFs, since yielding and energy dissipation are expected to occur only at the links, the links are the key members controlling the inelastic behavior of the system. Short links tend to yield due to shear, whereas long links tend to yield by flexure. The yield strength and deformation capacity of a link depend on whether it yields by shear or flexure. The remaining structural members, such as columns, beams outside the link, and braces, are referred to as non-dissipative members because they are expected to remain elastic even when the links reach their ultimate strength owing to material overstrength and strain-hardening effects. AISC 341 [1] requires that the design member force of non-dissipative members be determined by considering the capacity-limited seismic load effect, which is the member force that occurs when the links develop their ultimate strength. For this purpose, the link overstrength factor (or strain-hardening factor), Ω, is used, which is defined as the ratio of ultimate shear strength to expected yield strength of a link [2], as follows:

$$\Omega = \frac{V_u}{R_y V_n}, \tag{1}$$

where V_u is the ultimate shear strength, R_y is the material overstrength factor, and V_n is the nominal shear strength factor of a link.

Several researchers have conducted studies to determine the Ω factor of links. Okazaki and Engelhardt [3] and Okazaki et al. [4] conducted experimental studies using ASTM A992 wide flange sections (W-sections), obtaining Ω factors of up to 1.4. They found that Ω factor decreased as the link became slenderer. Azad and Topkaya [2] collected Ω factors of W-section links from previous experimental studies, as shown in Figure 1. As shown in the figure, the Ω factor of short links ($\rho < 1.0$) was greater than 1.5, while that of intermediate links ($\rho \approx 2$) appears to be less than 1.5. For long links, Ω = 1.5 can be considered a reasonable upper bound.

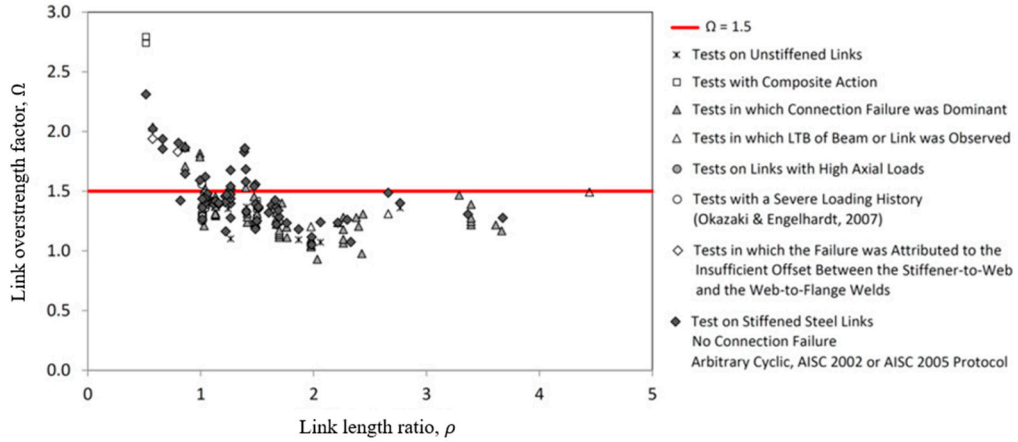

Figure 1. Link overstrength factor (Ω factor) values from previous experimental studies [2].

Roeder and Popov [5] and Popov and Engelhardt [6] proposed an Ω value of 1.5 for design purposes. The previous versions of the National Earthquake Hazards Reduction Program (NEHRP) [7] and AISC [8] used a value of 1.5 regardless of link length. Currently, AISC 341 [1] specifies a value of 1.25 for Ω factor. As the nominal strength and resistance factor are used in structural design, the effective Ω factor becomes 1.53 ($1.25R_y/\phi = 1.25 \times 1.1/0.9$), which is close to the experimentally obtained value of 1.5.

The design member forces of beams outside links and braces were determined by the force developed when the adjacent links on the same floor reach their ultimate strength. For columns, the design axial force should be the sum of the axial forces resulting from the overstrength of all links above the floor. However, not all links in a multi-story EBF develop their ultimate overstrength simultaneously. In light of this, AISC 341 [1] allows for a reduced Ω factor of 1.1 for column design in tall buildings.

Previous experimental and analytical studies have investigated the degree of simultaneous yielding in links. Whittaker et al. [9] performed shaking table tests on six-story EBF models and concluded that the possibility of the simultaneous yielding in all links was very low. Koboevic and Redwood [10] performed time history analyses on eight- and sixteen-story K-braced EBFs, demonstrating that the links on upper stories frequently yielded simultaneously, and that using a factor of 1.25 for the Ω factor would underestimate the axial forces of the upper floor columns. Subsequently, Richards [11] conducted a nonlinear time history analysis of a D-braced EBF and proposed values of 1.25 for columns in the first four stories below the top floor, 1.1 for the next 10 stories (if any), and 1.0 for the following 10 stories (if any). Richards [12] also found from similar nonlinear time history analysis results for an EBF with the chevron braces that the axial forces developed in the columns at the bottom story were only 55–70% of the estimated member force based on the capacity design principle.

Previous studies have indicated that the overstrength factor in the current provision tends to overestimate the axial forces in the lower-story columns, while it underestimates the axial forces in the upper-story columns. However, in previous studies, the analysis results and number of design variables considered are not sufficient to improve the current provision. In this study, we investigated the link overstrength factor of EBFs to verify the

capacity design principle. A large number of example buildings with different design variables, such as building height (number of stories), length-to-depth ratio of the links, and intensity of shaking (seismic design category), were used. To generate a sufficient number of design alternatives, an automated design algorithm based on a multi-objective optimization technique was applied. Nonlinear dynamic analyses were performed to verify compliance with the capacity design principle. Additionally, a link overstrength factor equation for column design in EBF systems was proposed based on analysis results.

2. Overview of EBF Systems

An EBF system comprises columns, braces, and beams, which are further divided into links and beams outside link. Figure 2 shows the plastic mechanism of a K-braced EBF, which is one of the most popular EBF systems. The design of an EBF system begins with the selection of link members, since the ultimate shear strength of the link affects the remaining non-dissipative members according to the capacity design concept. AISC 341 [1] specifies that the overstrength of links is basically 1.25 times the expected strength. However, for beams with floor slabs and columns in tall buildings, the overstrength factor can be reduced to 1.1 to account for the contribution of slabs to the yield strength and to account for the low possibility that all links above the story will yield simultaneously, respectively.

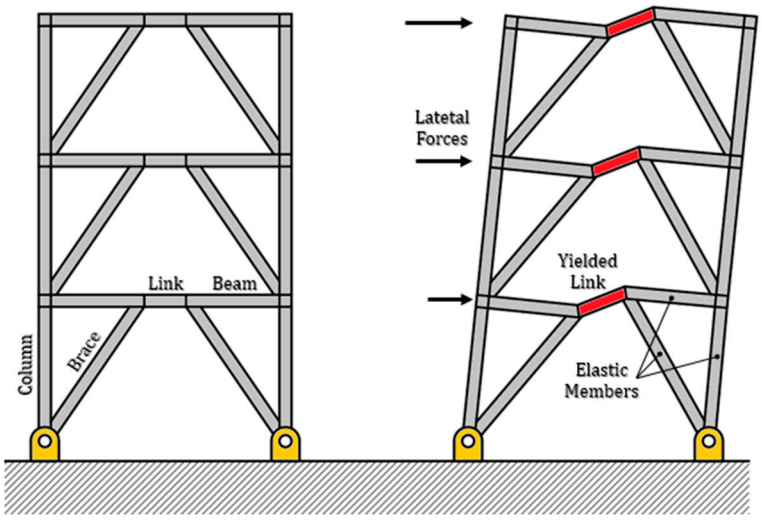

Figure 2. Plastic mechanism of a K-braced EBF.

The yielding behavior and deformation capacity of a link depend on its length. Shorter links tend to be governed by shear yielding, while longer links tend to be governed by flexural yielding. Thus, shorter links provide greater strength and a larger inelastic deformation capacity, whereas long links have the advantage of being able to freely place openings. In a K-braced frame, when the link is placed at the center of the bay, the moments at both ends of the link are identical. The relationship between shear force (V), end moment (M), and link length (e) can be represented by a simple equilibrium equation (see Figure 3), as follows:

$$e = \frac{2M}{V}, \tag{2}$$

Most design codes, including AISC 341 [1], SEAOC [13], and Eurocode 8 [14], classify links into three categories: "Short links" have a length ratio (ρ), as defined in Equation (3), of 1.6 or less; "long links" have a length ratio of 2.6 or more, as shown in Figure 4; and links in between are classified as "intermediate links", where the interaction between shear and moment is expected in the plastic range. In short links, energy dissipation occurs mainly

through the inelastic shear behavior of the link web. However, in long links, energy is dissipated mainly via plastic hinge formation at both ends of the link flanges.

$$\rho = \frac{e}{M_p / V_p}, \tag{3}$$

where M_p and V_p are the link plastic moment and plastic shear strengths, respectively.

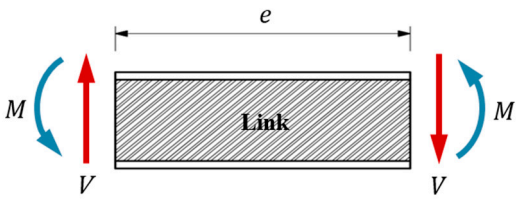

Figure 3. Free-body diagram of a link.

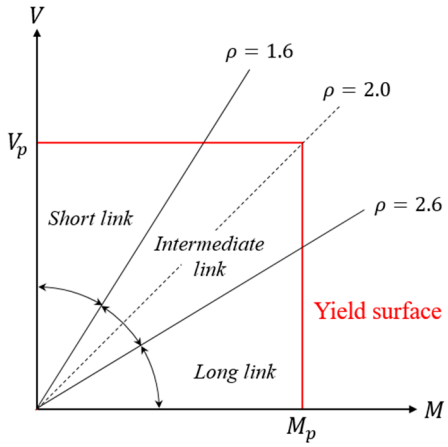

Figure 4. M–V interaction according to link length.

AISC 341 [1] states that when the ratio of axial force to the nominal yield strength ($=P/P_y$) is greater than 15%, the link length should be limited to prevent flange buckling; accordingly, the nominal strength is also reduced. However, for K-braced EBF systems, the effect of the axial force on the link is negligible because the horizontal component of the brace force is completely transmitted to the beam outside link in the form of an axial force [15,16]. The link's nominal shear strength (V_n), excluding the effect of axial forces, is defined as follows:

$$V_n = \min\left(V_p\,,\ \frac{2M_p}{e}\right), \tag{4a}$$

$$V_p = 0.6F_yA_w, \tag{4b}$$

$$M_p = F_yZ, \tag{4c}$$

where F_y denotes the specified minimum yield strength, Z is the plastic section modulus, and A_w is the web area of the link section.

Engelhardt and Popov [17] elucidated the correlation between ρ and the ultimate shear capacity of links using an M–V interaction curve. He suggested that the maximum shear and flexural strength were $1.5V_p$ and $1.5M_p$, respectively. A modification of Engelhardt's M–V interaction model is represented in Equation (5), which is used to relate the link length and overstrength factor due to shear alone. The overstrength factor resulting from the shear behavior is designated as Ω_v and plotted as a red line in Figure 5. Similarly, the M–V interaction model was modified in a different manner, as in Equation (6), to demonstrate the relationship between link length and the overstrength factor in terms of moment. The overstrength resulting from the flexural yielding is designated as Ω_m and represented by

the blue line in Figure 5. For a given length ratio, the actual overstrength factor is larger for these two values. As illustrated in Figure 5, the overstrength factor for short links governed by shear is 1.5, and for long links governed by flexure converges to 1.5. For an intermediate link, the overstrength factor is relatively low, which is likely due to the interaction between shear force and moment. The overall shape of the envelope of the two lines is similar to that shown in Figure 1, which represents the experimentally obtained overstrength factors. In this study, an approach to explain the overstrength factor using shear and flexural yielding was adopted for the analytical modelling of link behavior discussed in Section 4.1.

$$\frac{2\Omega_v}{3} = 1; \quad \text{for} \quad 0 \le \rho \le \frac{4}{3}, \tag{5a}$$

$$(\rho\Omega_v - 2)\sqrt{1 - \left(\frac{2\Omega_v}{3}\right)^2} + \left(\frac{2\Omega_v}{3}\right)^2 = 1; \quad \text{for } \rho \ge \frac{4}{3}, \tag{5b}$$

$$\frac{4\Omega_m}{3\rho} = 1; \quad \text{for} \quad 0 \le \rho \le \frac{4}{3}, \tag{6a}$$

$$2(\Omega_m - 1)\sqrt{1 - \left(\frac{4\Omega_m}{3\rho}\right)^2} + \left(\frac{4\Omega_m}{3\rho}\right)^2 = 1; \quad \text{for } \rho \ge \frac{4}{3}, \tag{6b}$$

where Ω_v and Ω_m are the overstrength factors of a link resulting from shear and flexural yielding, respectively.

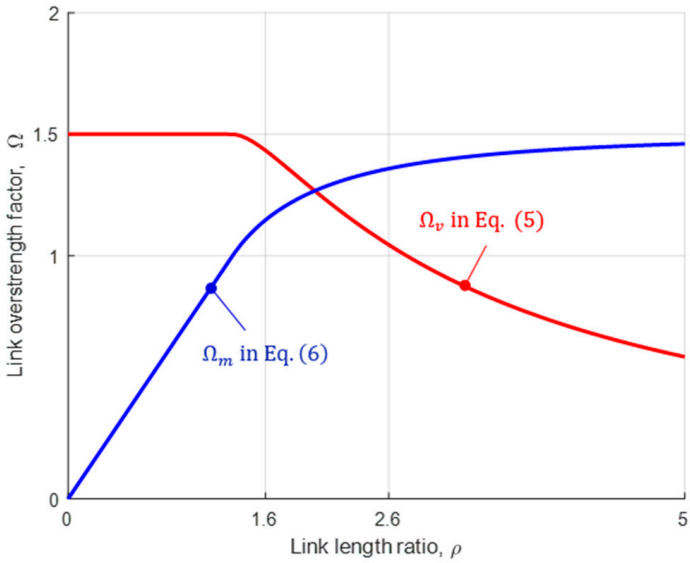

Figure 5. Theoretical link Ω factors.

The plastic deformation capacity of a link depends on its length ratio. The deformation capacity of short links is superior to that of long links. This phenomenon occurs because shear yielding occurs uniformly along the entire length of the member across the web section. By contrast, in the case of flexural yielding, plastic deformation is concentrated in the flanges at the ends of the member, which may lead to early local buckling. Accordingly, AISC 341 [1] specifies the permissible plastic rotation angle (θ_{pa}) in relation to the link length ratio, as shown in Figure 6. The link plastic rotation in EBFs (θ_p) can be obtained from the plastic story drift of the frame (Δ_p) in accordance with the simple plasticity theory (see Figure 7), as follows:

$$\theta_p = \frac{L}{e} \cdot \frac{\Delta_p}{h}. \tag{7}$$

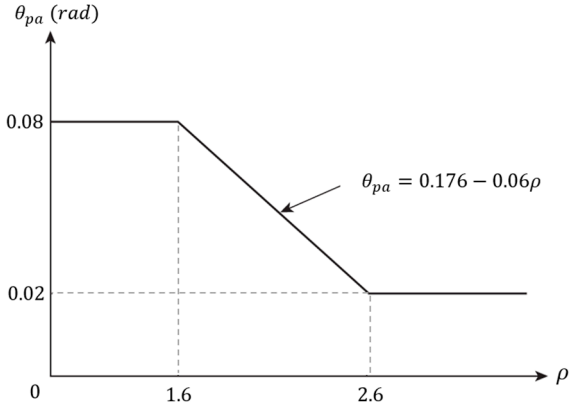

Figure 6. Allowable rotation angle according to the link length ratio.

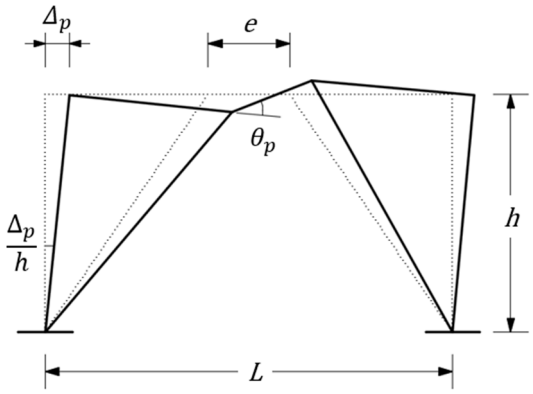

Figure 7. Deformed shape of a K-braced EBF.

3. Design of Example Buildings

3.1. Overview

Figure 8 shows the plan and elevation views of the example building. The example building has a plan consisting of 3 × 5 modules, with each unit having a square shape of 6 m × 6 m. All stories are 4 m in height. The K-braced EBF is located at the center of the exterior frame along the *x*-axis in all stories, as shown in Figure 8a. The beams, braces, and columns in the EBF are rigidly connected to one another. To ensure that the seismic load is resisted by the EBF only, the beams in the spans on either side of the EBF were hinge-connected to the columns. The effective seismic weight corresponding to 1.0DL + 0.25LL was considered in the analysis model. The red squares in Figure 8b represent the nodes where mass was assigned. In the *y*-axis direction, a moment-resisting frame was employed as the lateral-force-resisting system, which is not considered in this study.

The example buildings were assumed to be located in Seoul, South Korea, where the effective ground acceleration, S, is 0.176 g. The seismic design coefficients of the EBF system according to the KDS (Korea Design Standard) [18] ($R = 8$; $\Omega_0 = 2$; $C_d = 4$) were applied. The design member forces of the link members were determined via response spectrum analysis.

Various design conditions were considered, including the seismic design categories, height, width, and link length of the frames. Two site conditions of site classes A (hard rock) and D (stiff soil) were considered, resulting in two seismic design categories (SDCs), B and D, respectively. Furthermore, three building heights (5, 10, and 15 stories), three bay widths (6, 9, and 12 m), and three link span ratios (10%, 30%, and 50%) were considered. The variations in the design conditions are summarized into 54 performance groups and identified using the notation shown in Figure 9.

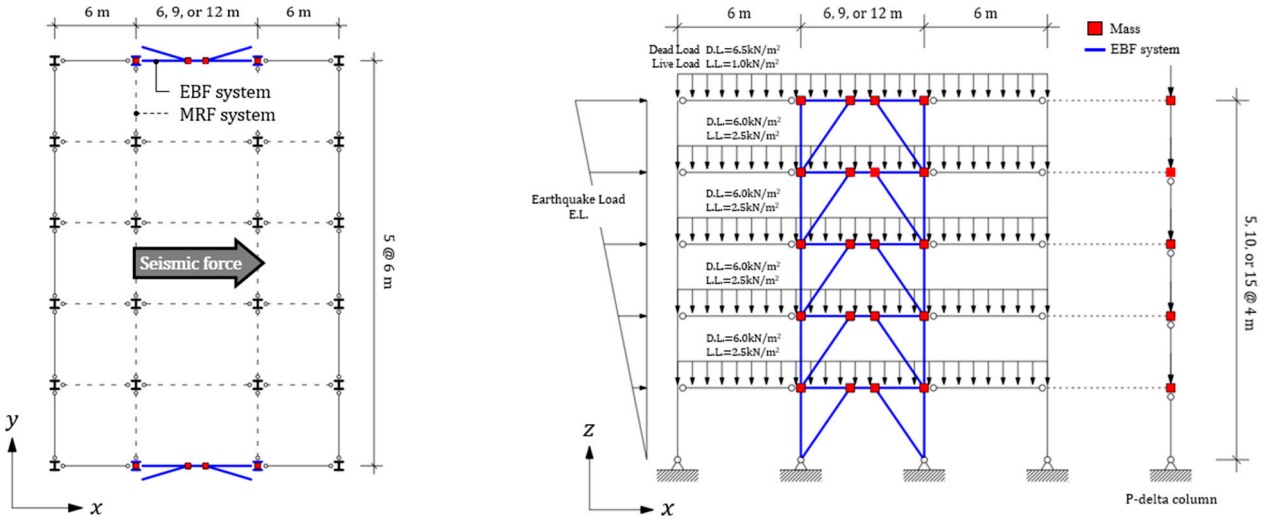

(**a**) (**b**)

Figure 8. Configuration of the example building: (**a**) plan view; (**b**) elevation view (*x*-axis direction).

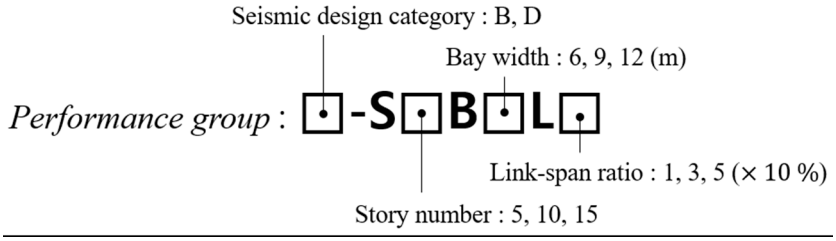

Figure 9. Notation used to identify the performance groups.

SM355 steel with a yield strength of 355 MPa was used for the columns, beams, and braces. It was assumed that the links had a constant length throughout the building height and the same cross section as the adjacent beams outside the links. W-shaped sections from the KS D 3502 section table [19] were used, and the members were grouped as listed in Table 1. The example building design in each performance group was facilitated by a multi-objective optimization technique described in detail in the next section.

Table 1. Member grouping of the example buildings.

Stories	Member	Level (Floor)														
		1	**2**	**3**	**4**	**5**	**6**	**7**	**8**	**9**	**10**	**11**	**12**	**13**	**14**	**15**
5	Column	C1			C2		C3									
	Beam	Bm1	Bm2	Bm3	Bm4	Bm5										
	Brace	Br1		Br2		Br3										
10	Column	C1				C2			C3		C4					
	Beam	Bm1		Bm2		Bm3			Bm4		Bm5					
	Brace	Br1		Br2			Br3			Br4						
15	Column	C1					C2			C3			C4		C5	
	Beam	Bm1				Bm2			Bm3			Bm4		Bm5		
	Brace	Br1			Br2			Br3			Br4			Br5		

3.2. Generation of Design Alternatives Using Multi-Objective Optimization

In general, structural members are selected to ensure safety and economic efficiency. Therefore, the optimal solution may not be unique. Furthermore, even under the same design conditions, the selection of structural members may vary depending on the designer's preferences. Multi-objective optimization techniques, which generate multiple optimal solutions, can be effective numerical procedures for accounting for this diversity in the design process.

In this study, a multi-objective metaheuristic algorithm based on NSGA-II (nondominated sorting genetic algorithm) was employed to generate multiple and varied design examples. The two objective functions used in the optimization are expressed in Equation (8a,b). The first objective function minimizes the sum of structural members. The second objective function maximizes the average value of the maximum demand-to-capacity ratios (DCRs) in member groups. The relevant constraints are appended, as shown in Equation (8c), which includes the condition that the demand strength cannot exceed the capacity of individual members, the width-to-thickness ratio requirement of the section, the link plastic rotation limitations, and the inter-story drift. Additionally, the conventional practice, in which the sections of columns on the lower story cannot be smaller than those on the upper story, was incorporated.

$$\textit{Minimize} \qquad f_1 = \sum_{i=1}^{N_{ele}} wA_iL_i + \sum_{j=1}^{N_{stf}} wV_{stf,j} \tag{8a}$$

$$\textit{Maximize} \qquad f_2 = \left[\frac{1}{N_{grp}} \sum_{i=1}^{N_{grp}} \left(\max_j \frac{R_{u,j}}{\phi R_{n,j}} \right)_i \right] \qquad j = 1, 2, \ldots, N_{ele,i} \tag{8b}$$

$$\textit{Subject to} \qquad \begin{gathered} R_u \le \phi R_n \\ b/t \le (b/t)_{limit} \\ \theta_p \le \theta_{pa} \\ \Delta_d/h \le \Delta_a/h \qquad \text{herein, } \Delta_d = \Delta_e C_d / I_E \\ d_{c,i} \le d_{c,i-1} \qquad i = 2, \ldots, N_{story} \end{gathered} \tag{8c}$$

where N_{ele}, N_{stf}, N_{story}, and N_{grp} are the total number of structural members, link web stiffeners, stories, and member groups in the EBF, respectively; A_i and L_i are the cross-sectional area and length of the structural member, respectively; $V_{stf,j}$ is the stiffener volume; w is the material's unit density; ϕ is the resistance factor; R_u and R_n are the demand and capacity, respectively, in terms of the generic strength, including the axial force, shear force, and moments; b/t is the width-to-thickness ratio; θ_p is the link plastic rotation, which can be estimated using Equation (7), where θ_{pa} is the allowable value; $d_{c,i}$ indicates the column member dimensions on the i-th story; Δ_d/h is the design inter-story drift evaluated using the inter-story displacement from elastic analysis Δ_e, the displacement amplification factor C_d, and the importance factor I_E of the building; finally, Δ_a/h is the allowable inter-story drift specified in the design code.

In the design of the EBF system, the link members are first determined based on elastic analysis results. Next, the design forces (i.e., demand) of the non-dissipative members are determined by incorporating the capacity-limited seismic load effect, which corresponds to the member forces of the non-dissipative members when the links have reached their ultimate strength (fully yielded and strain-hardened). Nevertheless, the member forces resulting from the inelastic behavior cannot be directly obtained via elastic analysis. Therefore, an additional analysis representing the post-yielding state of the structure, as illustrated in Figure 10, was performed to obtain the member forces due to the capacity-limited seismic load effect [16]. In the model depicted in Figure 10, the link elements were cut at their center, and roller supports were placed on the outer sides of the frame to prevent side sway. In accordance with AISC 341 Section F3.3, the drift-induced flexural forces in the columns were neglected to allow for a straightforward derivation of the design forces of non-dissipated members. It should be noted that no external forces are applied except for the shear forces at the cut section (at the center of link members), which correspond to the internal force of the link at the center. It is evident that the design forces of the beams

or diagonal braces can be estimated directly from the ultimate strength of the adjacent links. However, the axial forces of the columns should be estimated by considering the vertical shear forces of the links at the floors above. Both the initial elastic analysis (to obtain the member forces of the link members) and subsequent analysis (to obtain the design member forces of the non-dissipative members) were performed using OpenSees [20], an object-oriented open-source software framework.

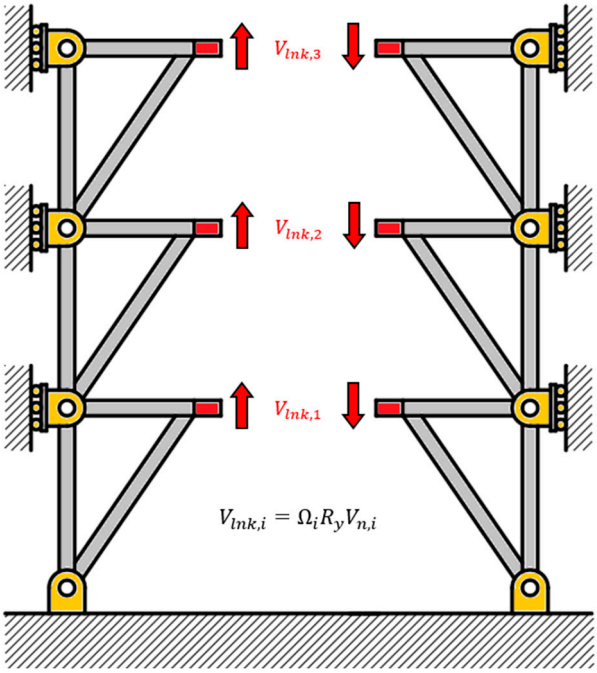

Figure 10. Analysis model for the design force of non-dissipative members.

The aforementioned optimization algorithm was implemented using MATLAB R2022b [21]. For iterative computation, a MATLAB routine was devised to interactively modify the OpenSees input file for elastic analyses. Figure 11 shows the progress of optimization for the D-S15B9L1 performance group as an example. The vertical and horizontal axes represent the first and second objective functions, respectively. The solutions connected by a red line indicate the Pareto front, which represents a set of the best solutions for the given objective functions. As the evolution of the generation proceeded, the Pareto front moved leftward and downward, indicating that the solution approached the optimal state. In the NSGA-II used in this study, one generation consisted of 100 populations and the optimization was terminated at the 200th, 250th, and 300th generation for the five-, ten-, and fifteen-story EBFs, respectively. Once the computations are completed, the solutions on the Pareto front are selected as the final solutions. At most, ten solutions were obtained for each performance group. Figure 12 shows a comparison between the final design alternatives in terms of structural quantity. As expected, the structural quantity increases as the bay width and number of stories increase.

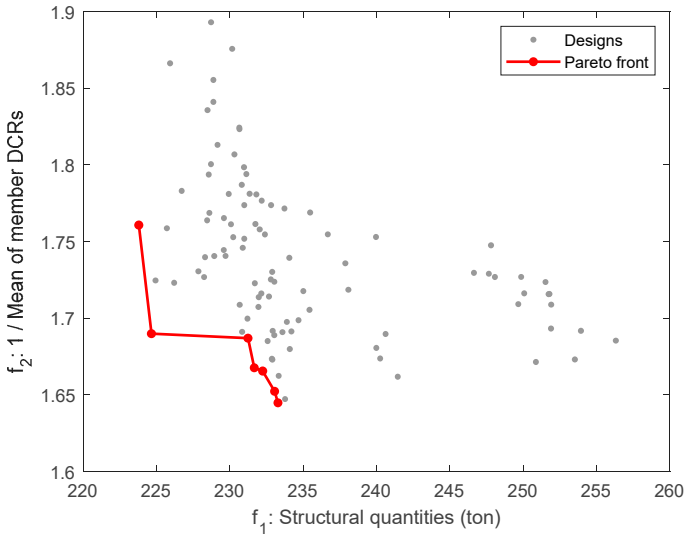

Figure 11. Optimization results (D-S15B9L1 performance group).

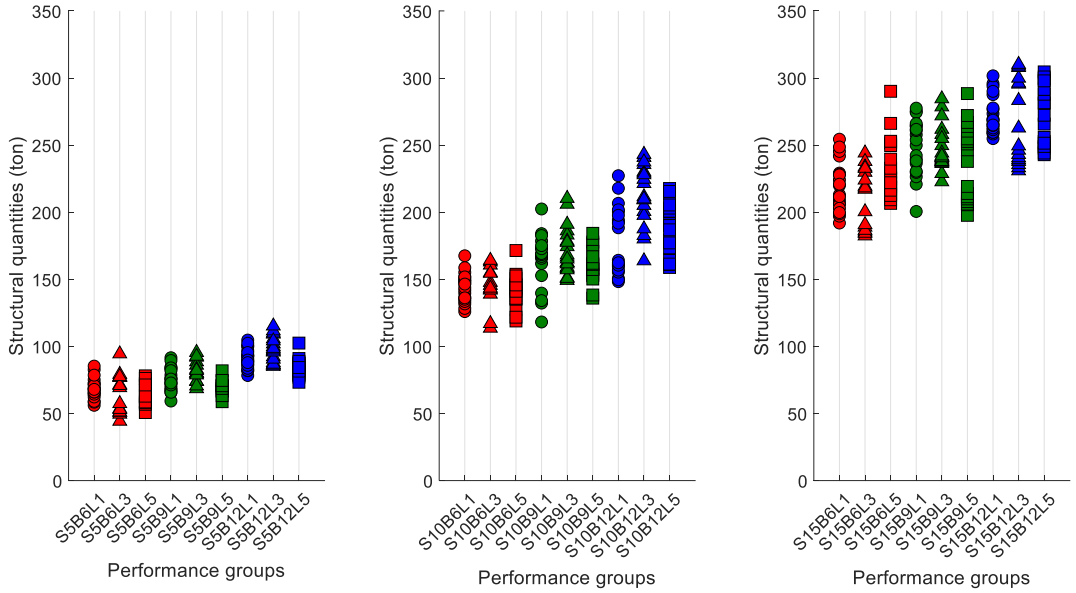

(**a**) (**b**) (**c**)

Figure 12. Structural quantities by performance group: (**a**) five-story building; (**b**) ten-story building; (**c**) fifteen-story building.

4. Structural Analysis

4.1. Nonlinear Analysis Model

In this section, nonlinear analyses are performed to ascertain whether the concept of capacity design principle is satisfied (i.e., whether the non-dissipative member yields) and to identify the link overstrength factor necessary to prevent the non-dissipative member from yielding. To conduct nonlinear analyses, the elastic analysis models obtained using the numerical procedure based on the multi-objective optimization described in the previous section were transformed into nonlinear models.

Only the EBF frames were explicitly modeled, whereas the gravity frames were lumped into leaning columns to represent the P-delta effect. Nonlinear properties were modeled exclusively at the links because nonlinear behavior is expected only at these links based on the capacity design principle. Nonlinear time history analyses were conducted using OpenSees [20].

Several modeling approaches [22–30] have been proposed to simulate the nonlinear shear and flexural behaviors of links. In this study, a link model based on Engelhardt's interaction model [17] was adopted. As shown in Figure 13, the link model consisted of a link beam (LB), two translational springs (TSs), and two rotational springs (RSs). The length of the LB is identical to that of the actual link and is modeled as a rigid beam element because the elastic stiffness is already accounted for in the springs. The TSs and RSs are zero-length elements that simulate nonlinear shear and flexural behavior, respectively. A bilinear material model (Steel01) in OpenSees [20] was used for the TS and RS components. Table 2 presents the nonlinear modeling properties of the spring elements. The notation used in Table 2 is also shown in Figure 14.

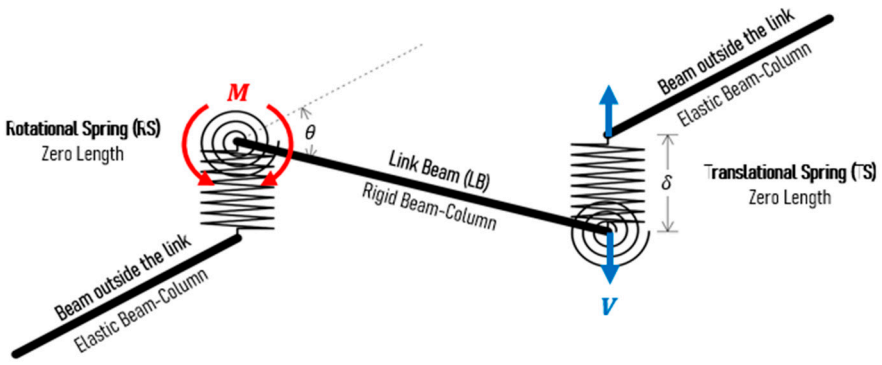

Figure 13. Analytical model for link members.

Table 2. Nonlinear properties of the spring elements.

Element	Yield Strength	Elastic Stiffness	Yield Deformation	Ultimate Plastic Deformation	Ultimate Overstrength Factor	Strain Hardening Ratio
TS	$V_{pe} = R_y V_p$	$K_v = \frac{2GA_w}{e}$	$\delta_y = \frac{V_{pe}}{K_v}$	$\delta_{pu} = 0.08 \times \frac{e}{2}$	$\Omega_{vu} = \frac{V_u}{R_y V_p} = 1.5$	$b_v = \frac{(\Omega_{vu}-1)V_{pe}}{K_v \delta_{pu}}$
RS	$M_{pe} = R_y M_p$	$K_m = \frac{6EI}{e}$	$\theta_y = \frac{M_{pe}}{K_m}$	$\theta_{pu} = 0.02$	$\Omega_{mu} = \frac{M_u}{R_y M_p} = 1.5$	$b_m = \frac{(\Omega_{mu}-1)M_{pe}}{K_m \theta_{pu}}$

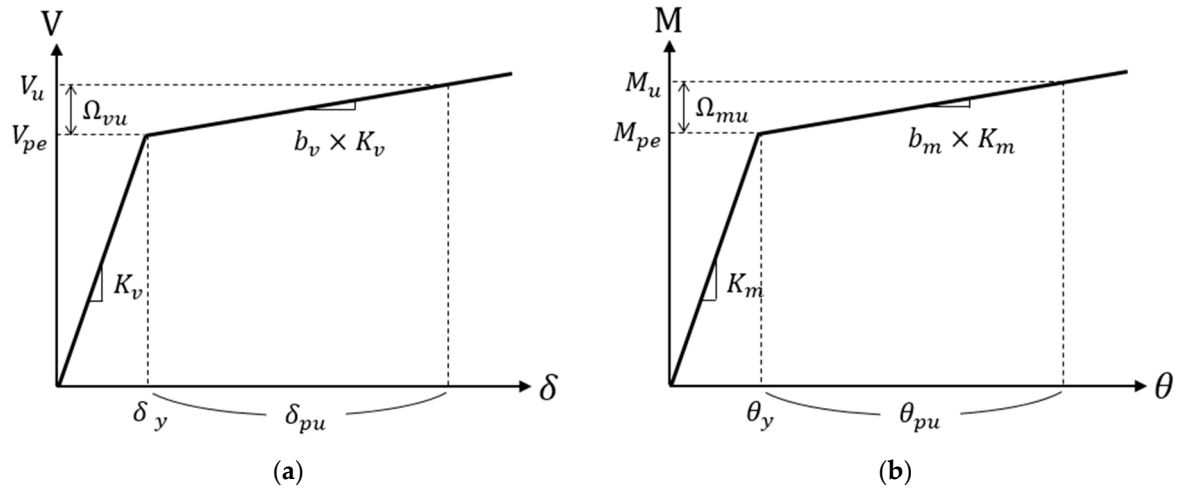

Figure 14. Load–displacement relationship of the link: (**a**) TS element; (**b**) RS element.

The expected yield strengths of the TS and RS elements, V_{pe} and M_{pe} in Figure 14, respectively, were calculated using Equation (4b,c), respectively. In the case of short links, which are governed by shear yielding, the TS element attains its ultimate strength, including strain-hardening behavior, while the RS element remains elastic. In the case of long links,

the TSs and RSs behave in a manner opposite to that observed in short links. The ultimate plastic rotations for the TSs and RSs were set as 0.08 and 0.02 rad, respectively. These values are identical to the allowable plastic rotation angles for short and long links, as specified in AISC 341 [1] (Figure 6).

In the case of intermediate links, shear and moment yielding can occur simultaneously. Given that the shear and moment are in equilibrium, if yielding occurs in either of these and the strength increases owing to strain hardening, subsequent yielding occurs in the other. Consequently, the final Ω factor at the instant of link failure becomes less than 1.5. These behaviors are consistent with the observations discussed in Section 2 (Figure 5).

4.2. Nonlinear Dynamic Analysis

In the nonlinear dynamic analysis, ten earthquake records, consisting of five historical and five artificial earthquake records, were used for each SDC (Figure 15). The selected historical earthquakes are listed in Table 3. For artificial earthquakes, EqMaker [31] was used to generate the time histories for SDC B and D, with the relevant parameters specified in the KDS.

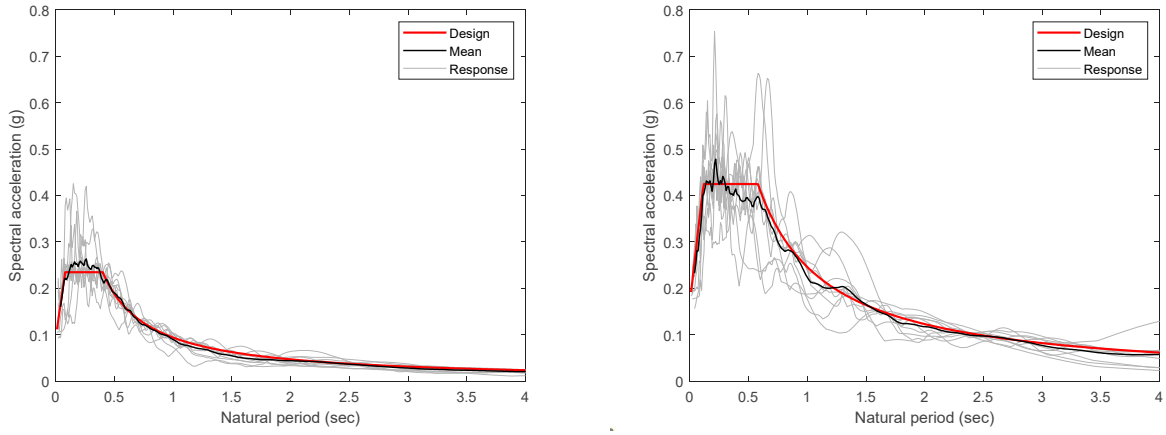

Figure 15. Spectral accelerations of the selected earthquakes: (**a**) SDC B; (**b**) SDC D.

Table 3. List of historical earthquakes.

SDC	Event	Station	Year	Magnitude
B	Superstition Hills	Poe Road (temp)	1987	6.5
	Duzce, Turkey	Bolu	1999	7.1
	San Fernando	LA—Hollywood Stor	1971	6.6
	Imperial Valley	El Centro Array #11	1979	6.5
	Manjil, Iran	Abbar	1990	7.4
D	Landers	Yermo Fire Station	1992	7.3
	Kocaeli, Turkey	Arcelik	1999	7.5
	Kobe, Japan	Shin-Osaka	1995	6.9
	Loma Prieta	Gilroy Array #3	1989	6.9
	Northridge	Canyon Country-WLC	1994	6.7

The purpose of the nonlinear time history analyses is to capture the limit state of each structure and investigate the overstrength demand for the links. The link plastic rotation and story drift were chosen as the engineering demand parameters describing the state of the structure. In this study, a numerical technique based on the line search

was used to minimize the number of nonlinear analyses required to reach the limit state. The nonlinear time history analysis was repeated with different scaling factors until the condition specified in Equation (9) was satisfied. In Equation (9), the first and second terms in the parentheses indicate the criteria for link rotation and inter-story drift, respectively.

$$1.00 < \text{Max}\left(\frac{\theta_{p,max}}{\theta_{pa}}, \frac{\Delta_{max}}{\Delta_a}\right) < 1.01, \tag{9}$$

where $\theta_{p,max}$ is the maximum link plastic rotation angle in the response history and θ_{pa} is the allowable plastic rotation specified in AISC 341 [1]. Similarly, Δ_{max} is the maximum inter-story drift in the response histories and Δ_a is the allowable inter-story drift corresponding to the collapse prevention level for braced frames as defined in FEMA 356 [32].

Figure 16 illustrates the progress of iterations in the dynamic analysis using the line search method in the case of B-S15B9L1 as an example. An initial guess of 0.5 g was chosen for the maximum PGA (peak ground acceleration). After the first iteration, the PGA for the second iteration was determined based on the maximum link plastic rotation or the story drift recorded in the first iteration. As shown in Figure 16, the link plastic rotation was the dominant parameter rather than the inter-story drift, and the structure reached its limit state after six iterations.

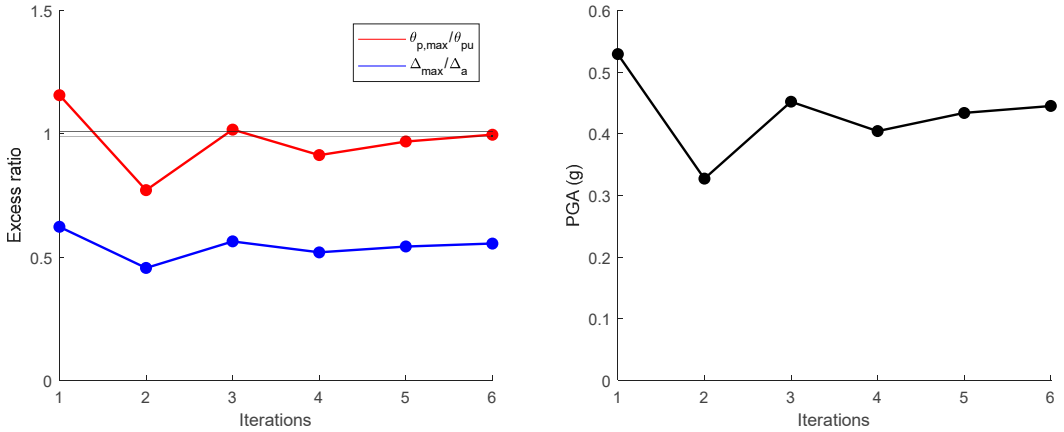

(**a**) (**b**)

Figure 16. Convergence process of the dynamic analysis (for B-S15B9L1): (**a**) link plastic rotation and inter-story drift; (**b**) PGA.

The overall procedure is similar to that of the incremental dynamic analysis (IDA), which is commonly used to assess the seismic performance of structures [33]. However, unlike IDA, the PGA value corresponding to collapse is not considered important in this study. The aim of the analyses is to capture the limit state of the structure for a given time history record and investigate the DCR distribution throughout the structure to determine the link overstrength demand, as described next.

5. Analysis Results

Overstrength Demand

As mentioned previously, the link overstrength factor is used to determine the design forces of non-dissipative members. The design forces of beams outside link and braces can be determined directly from the link shear force on the same story. The analysis results were used to calculate the overstrength demand by dividing the maximum link shear force by their expected shear strength, as follows:

$$\Omega_{b,i} = \max\left[\text{abs}\left(\frac{V_i(t)}{R_y V_{n,i}}\right)\right], \tag{10}$$

where V_i is the shear force acting at the ends of the link (on the ith story), R_y is the material overstrength factor, and $V_{n,i}$ is the nominal link shear strength (on the ith story).

Figure 17 shows the link overstrength demand for the design of beams outside link and braces for the five-, ten-, and fifteen-story buildings. Each light-gray line depicts the overstrength demand in a single time history response; therefore, the value varies across stories. However, the maximum values in all time history responses (dark dots in Figure 17) reached 1.5 in all stories, which was expected, as the analytical link models (Figure 13) were established such that the maximum link strength was 1.5 times its yield strength. Therefore, a value of 1.5, which is equivalent to Ω factor of 1.25 in AISC 341 [1] for the design of beams outside link and braces, is reasonable.

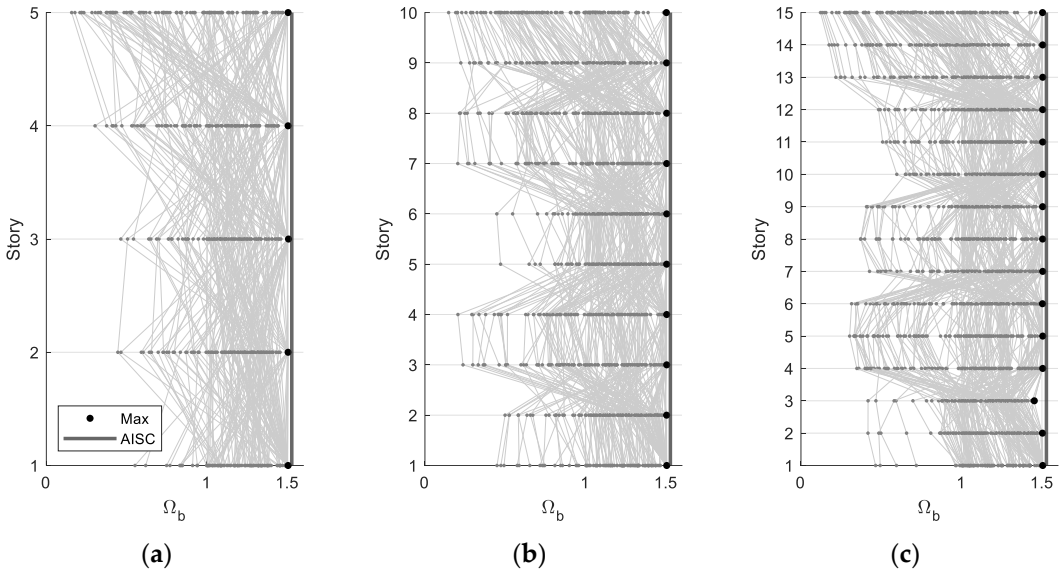

Figure 17. Link overstrength demands for design of beams outside link and braces: (**a**) five-story building; (**b**) ten-story building; (**c**) fifteen-story building.

However, the design axial forces of the columns should be the sum of the axial forces resulting from the overstrength of all links on the floors above. Therefore, the overstrength demands for column design, Ω_c, were calculated based on the analysis results. The Ω_c value for the ith story is defined as the peak value obtained from the cumulated shear force of the upper links, normalized by the sum of their expected strengths, as follows:

$$\Omega_{c,i} = \max\left[\text{abs}\left(\frac{\sum_{j=i}^{N_{story}} V_j(t)}{R_y \sum_{j=i}^{N_{story}} V_{n,j}}\right)\right]. \quad (11)$$

The results obtained using Equation (11) are shown in Figure 18, and their maximum values are listed in Table 4. The Ω factors from AISC 341 [1] and Richards [11] are also shown as solid and dashed black lines, respectively, for comparison. It is worth noting that the Ω factors from AISC 341 [1] and Richards [11] were scaled by multiplying them by the material overstrength factor (R_y = 1.1) and divided by the resistance factor (ϕ = 0.9). Accordingly, the Ω factor of 1.1 according to AISC 341 [1], which is typically used for tall buildings, was converted to approximately 1.34.

As can be seen in Figure 18, the overstrength demands for column design are greater than the AISC 341 factor (Ω = 1.1) in all stories for the five-story frame and in the upper stories for the ten- and fifteen-story frames. The Ω factors from Richards [11] have a value of 1.25 for the top four stories, which appears to be reasonable compared with the analysis results. However, in the 10th and 11th stories of the 15-story building, the Ω_c demands exceeded Richards's factor. In the lower stories of the 10- and 15-story frames, the Ω_c

demands became significantly smaller, making the Ω factors of both AISC 341 [1] and Richards [11] appear overly conservative.

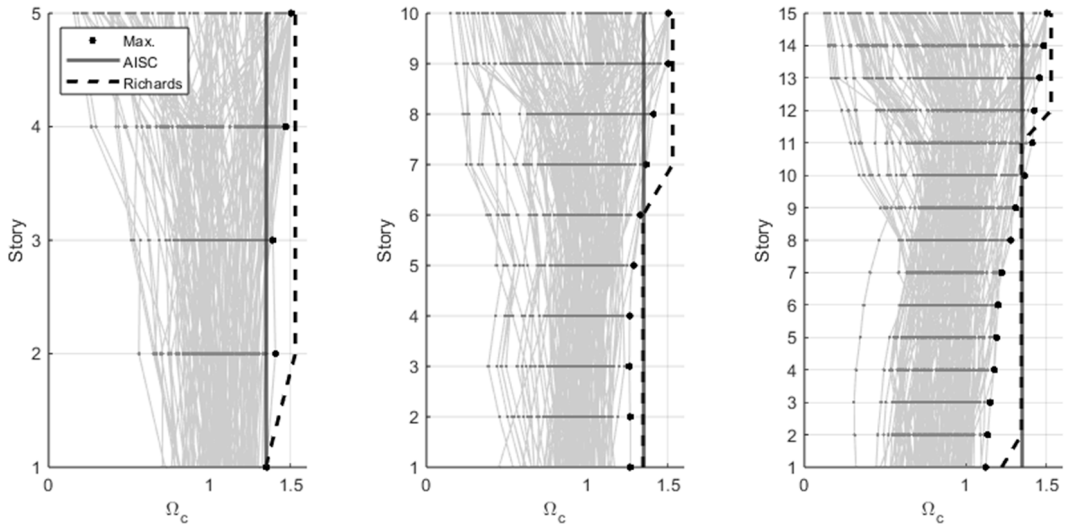

Figure 18. Ω_c factor from nonlinear dynamic analysis results: (**a**) five-story building; (**b**) ten-story building; (**c**) fifteen-story building.

Table 4. Maximum demands of Ω_c.

	Five-Story Building	Ten-Story Building	Fifteen-Story Building
1F	1.345	1.263	1.120
2F	1.400	1.262	1.133
3F	1.384	1.257	1.149
4F	1.464	1.259	1.173
5F	1.500	1.284	1.187
6F		1.325	1.197
7F		1.361	1.219
8F		1.406	1.275
9F		1.497	1.306
10F		1.500	1.359
11F			1.407
12F			1.421
13F			1.453
14F			1.479
15F			1.500

6. Proposed Overstrength Factors for Column Design

The overstrength demands for columns (Ω_c) were relatively small in the lower stories because the probability of simultaneous yielding (actually developing their full capacity) of all links in the upper stories is low. However, the current AISC 341 [1] does not account for this phenomenon, which can lead to overdesign of columns in lower stories. Therefore, an equation representing the overstrength factor for column design is proposed based on the analysis results.

First, the effects of SDC, bay width, and link span ratio on the overstrength demands were investigated, and the results are shown in Figure 19. As can be seen, the maximum demand does not show significant differences despite differences in the design variables.

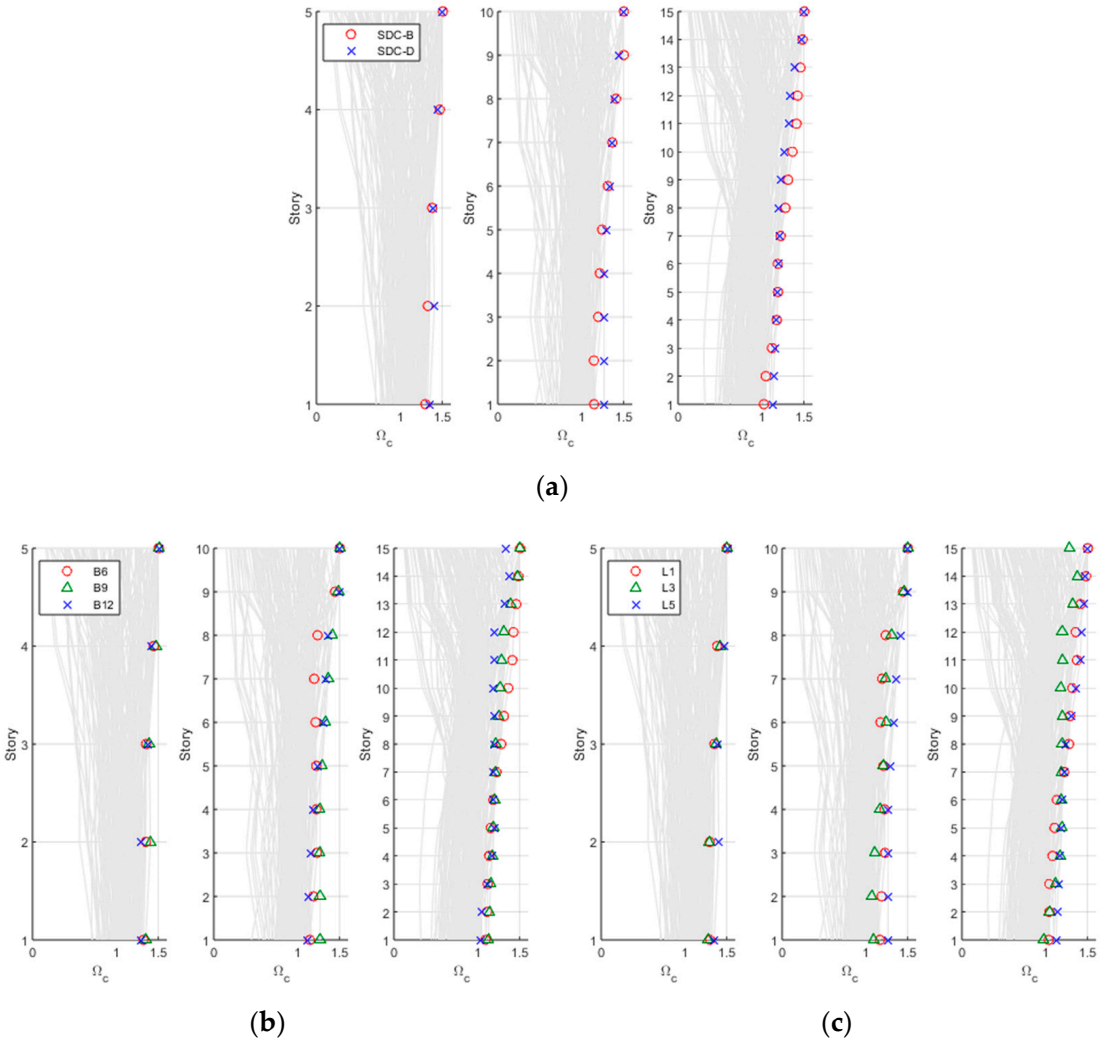

(**a**)

(**b**) (**c**)

Figure 19. Effects of the SDC, bay width, and link span ratio on Ω_c: (**a**) SDC B and D; (**b**) bay width (6, 9, and 12 m); (**c**) link span ratio (10%, 30%, and 50%).

From the regression analyses of the maximum overstrength demand shown in Figure 18 and Table 4, an equation for Ω_c was proposed as follows:

$$\Omega_{c,i} = 1.50 - 0.025\left(N_{story} - i\right) \geq 1.15, \tag{12}$$

where N_{story} is the number of stories and i is the column location.

Figure 20 compares the Ω_c factors from the proposed equation with the maximum demands from the analysis results. As can be seen, the Ω_c demands decrease almost linearly from the top to the bottom stories. As the slopes of the regression equation results for the five-, ten-, and fifteen-story frames were similar, a constant slope was used in the equation regardless of the number of stories. A lower bound, similar to the minimum value in Table 4, was set to prevent excessively small values in high-rise buildings.

To validate the proposed equation, a new set of example buildings was generated. New Ω_c factors multiplied by R_y/ϕ instead of the AISC factor were applied and similar nonlinear analyses as those described in Section 4 were performed. Figure 21a shows the structural quantities for the performance group of D-S15B9L1. When the EBFs were

designed using the proposed equation, the structural quantities averaged for 100 example buildings was 140.8 tons, which is 18.9% and 14.3% lower than those obtained using the AISC 341 [1] and Richards [11] equations, respectively. Figure 21b shows the DCR values of the EBF members designed using the proposed equation based on the dynamic analysis results. As shown in the figure, the DCRs of the members did not exceed unity, indicating that yielding of any non-dissipative members did not occur. Consequently, by using the proposed Ω_c factors, the structural quantities of the EBF system were reduced while satisfying the capacity design principle.

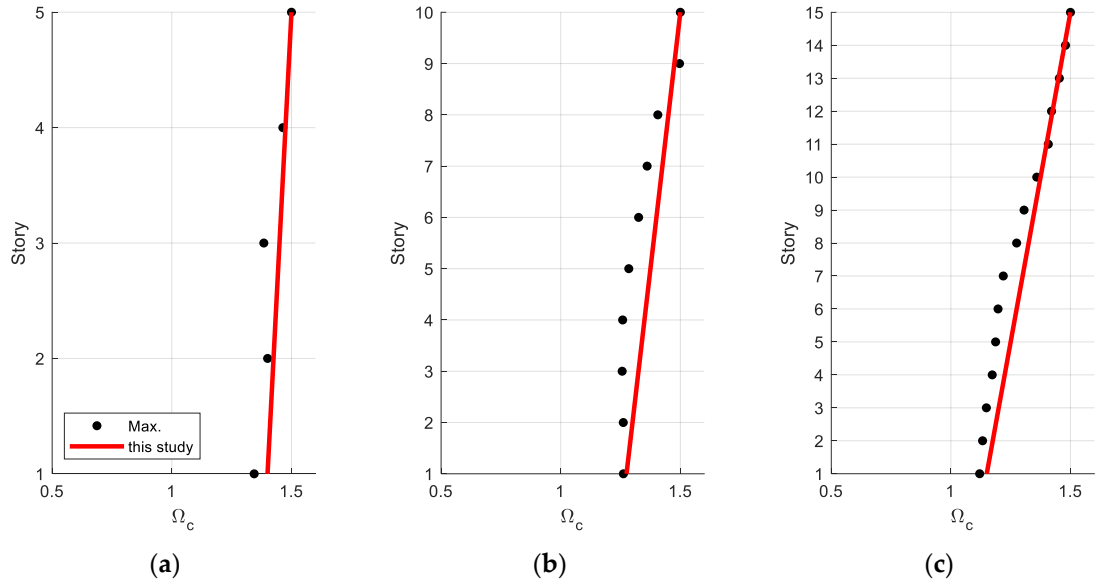

Figure 20. Performance of the EBFs designed using the proposed equation (D-S15B9L1): (**a**) five-story building; (**b**) ten-story building; (**c**) fifteen-story building.

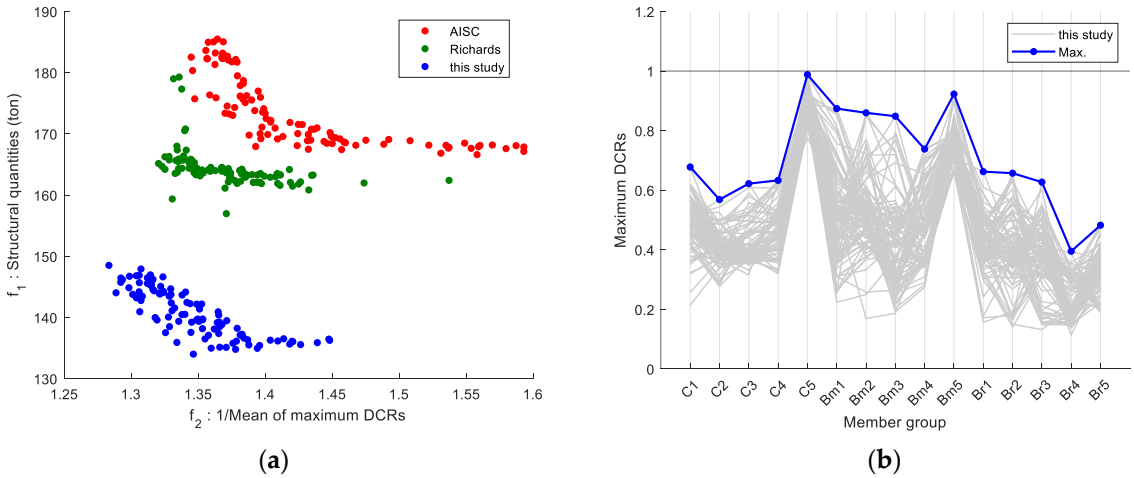

Figure 21. Performance of the EBFs designed using the proposed equation (D-S15B9L1): (**a**) objective space of the design examples; (**b**) maximum DCRs of the member groups.

7. Conclusions

In EBFs, inelastic deformation owing to seismic loads is only permitted in the links. The remaining structural members, such as columns, beams outside link, and braces, are called non-dissipative members and are designed using the capacity design concept so that they remain elastic even when the links are fully yielded and strain-hardened. For this purpose, the link overstrength factor, Ω, is used in the design of non-dissipative members,

and is defined as the ratio of the ultimate shear strength of a link to its expected strength. AISC 341 specifies a value of 1.1 for the Ω factors of links for column design regardless of the number of stories. However, as the number of stories increases, the probability of simultaneous yielding decreases, and the axial force of columns in tall buildings may be overestimated.

In this study, the relevance of the current Ω factor for EBF systems was investigated through nonlinear analyses of example buildings. A sufficient number of example buildings was used to include the influence of variability owing to design conditions and designer preferences. Various design conditions were considered, including different seismic design categories (SDC B and D), building heights (5, 10, or 15 stories), bay widths (6, 9, or 12 m), and link lengths (10%, 30%, and 50% of the bay width), which resulted in 54 performance groups. Additionally, to account for the variability in member selection due to designer preferences, multiple design alternatives were included in the example buildings under the same performance group. An automated design algorithm based on a multi-objective optimization technique was applied to generate multiple design alternatives. A total of 471 example buildings were generated and used for nonlinear dynamic analysis to evaluate Ω factors. In the nonlinear model, two types of zero-length spring elements were positioned at the link ends to simulate the inelastic behavior in shear and flexure. In the nonlinear time history analyses, an iterative method was used to accurately capture the limit state of the structure. The distribution of demand-to-capacity ratios (DCRs) throughout the structure was investigated to determine the link overstrength demand. The results indicated that it is reasonable to use the current Ω factor for beam outside link and brace design; however, the current Ω factor leads to an overestimation of axial force in columns, especially in the lower stories of tall buildings. Through regression analysis, a new Ω factor equation for column design was proposed. It was demonstrated that the structural quantities of the 15-story frames designed using the proposed equation were reduced by an average of 19% compared to those designed using the current Ω factor.

Author Contributions: Conceptualization, Y.H. and E.Y.; methodology, Y.H.; software, Y.H.; validation, Y.H.; formal analysis, Y.H.; investigation, Y.H. and E.Y.; resources, Y.H.; data curation, Y.H.; writing—original draft preparation, Y.H.; writing—review and editing, E.Y.; visualization, Y.H.; supervision, E.Y.; project administration, E.Y.; funding acquisition, E.Y. All authors have read and agreed to the published version of the manuscript.

Funding: This research was funded by a grant (2022-MOIS63-003(RS-2022-ND641021)) of Cooperative Research Methods and Safety Management Technology in National Disasters funded by the Ministry of Interior and Safety (MOIS, Republic of Korea).

Institutional Review Board Statement: Not applicable.

Informed Consent Statement: Not applicable.

Data Availability Statement: The original contributions presented in the study are included in the article, further inquiries can be directed to the corresponding author.

Acknowledgments: This research was supported by a grant (2022-MOIS63-003(RS-2022-ND641021)) of Cooperative Research Methods and Safety Management Technology in National Disasters funded by the Ministry of Interior and Safety (MOIS, Republic of Korea).

Conflicts of Interest: The authors declare no conflicts of interest.

References

1. *ANSI/AISC 341-22*; Seismic Provisions for Structural Steel Buildings. American Institute of Steel Construction: Chicago, IL, USA, 2022.
2. Azad, S.K.; Topkaya, C. A review of research on steel eccentrically braced frames. *J. Constr. Steel Res.* **2017**, *128*, 53–73. [CrossRef]
3. Okazaki, T.; Engelhardt, M.D. Cyclic loading behavior of EBF links constructed of ASTM A992 steel. *J. Constr. Steel Res.* **2007**, *63*, 751–765. [CrossRef]
4. Okazaki, T.; Arce, G.; Ryu, H.C.; Engelhardt, M.D. Experimental study of local buckling, overstrength, and fracture of links in eccentrically braced frames. *J. Struct. Eng.* **2005**, *131*, 1526–1535. [CrossRef]

5. Roeder, C.W.; Popov, E.P. *Inelastic Behavior of Eccentrically Braced Steel Frames Under Cyclic Loadings*; NASA STI/Recon Technical Report N. Earthquake Engineering Research Center: Berkeley, CA, USA, 1977; Volume 78, p. 20375.
6. Popov, E.P.; Engelhardt, M.D. Seismic eccentrically braced frames. *J. Constr. Steel Res.* **1988**, *10*, 321–354. [CrossRef]
7. Building Seismic Safety Council. *Recommended Provisions for the Development of Seismic Regulations for New Buildings: Commentary*; National Earthquake Hazards Reduction Program: Washington, DC, USA, 1985; Volume 17.
8. American Institute of Steel Construction. *Tentative Seismic Provisions*; American Institute of Steel Construction: Chicago, IL, USA, 1989.
9. Whittaker, A.S.; Uang, C.M.; Bertero, V.V. *Earthquake Simulation Tests and Associated Studies of a 0.3-Scale Model of a Six-Story Eccentrically Braced Steel Structure*; Earthquake Engineering Research Center: College of Engineering, University of California: Berkeley, CA, USA, 1987.
10. Koboevic, S.; Redwood, R. Design and seismic response of shear critical eccentrically braced frames. *Can. J. Civ. Eng.* **1997**, *24*, 761–771. [CrossRef]
11. Richards, P.W. *Cyclic Stability and Capacity Design of Steel Eccentrically Braced Frames*; University of California: San Diego, CA, USA, 2004.
12. Richards, P.W. Seismic column demands in ductile braced frames. *J. Struct. Eng.* **2009**, *135*, 33–41. [CrossRef]
13. Structural Engineers Association of California (SEAOC). *Recommended Lateral Force Requirements and Tentative Commentary*; Structural Engineers Association of California (SEAOC): Sacramento, CA, USA, 1988.
14. *EN 1998–1: 2005*; Eurocode 8: Design of Structures for Earthquake Resistance. Part, 1. CEN: Brussels, Belgium, 2005.
15. Becker, R.; Ishler, M. *Seismic Design Practice for Eccentrically Braced Frames*; Structural Steel Educational Council: Moraga, CA, USA, 1996; 27p.
16. Eng, M.B.P.D.; Uang, C.M.; SE, R.S. *Ductile Design of Steel Structures*; McGraw-Hill Education: New York, NY, USA, 2011.
17. Engelhardt, M.D.; Popov, E.P. *Behavior of Long Links in Eccentrically Braced Frames*; Report No. UCB/EERC-89/01; Earthquake Engineering Research Center: University of California: Berkeley, CA, USA, 1989.
18. *KDS 41 17 00*; Seismic Design Code for Buildings. Ministry of Land, Infrastructure and Transport of Korea: Sejong, Republic of Korea, 2019.
19. *KS D 3502:2021*; Dimensions, Mass and Permissible Variations of Hot Rolled Steel Sections. KATS: Eumseong-gun, Republic of Korea, 2022.
20. Mazzoni, S.; McKenna, F.; Scott, M.H.; Fenves, G.L. *OpenSees Command Language Manual*; Pacific Earthquake Engineering Research (PEER) Center: Berkeley, CA, USA, 2006; Volume 264, pp. 137–158.
21. The MathWorks Inc. *MATLAB Version: 9.13.0 (R2022b)*; The MathWorks Inc.: Natick, MA, USA, 2022.
22. Ramadan, T.; Ghobarah, A. Analytical model for shear-link behavior. *J. Struct. Eng.* **1995**, *121*, 1574–1580. [CrossRef]
23. Richards, P.; Uang, C.M. *Development of Testing Protocol for Short Links in Eccentrically Braced Frames*; Department of Structural Engineering, University of California: San Diego, CA, USA, 2003.
24. Rozon, J.; Kovoebic, S.; Tremblay, R. Study of global behavior of eccentrically braced frames in response to seismic loads. In Proceedings of the 14th World Conference on Earthquake Engineering, Beijing, China, 12–17 October 2008.
25. Malakoutian, M.; Berman, J.W.; Dusicka, P. Seismic response evaluation of the linked column frame system. *Earthq. Eng. Struct. Dyn.* **2013**, *42*, 795–814. [CrossRef]
26. Moghaddasi, B.N.S.; Zhang, Y. Seismic analysis of diagrid structural frames with shear-link fuse devices. *Earthq. Eng. Eng. Vib.* **2013**, *12*, 463–472. [CrossRef]
27. O'Reilly, G.J.; Sullivan, T.J. Direct displacement-based seismic design of eccentrically braced steel frames. *J. Earthq. Eng.* **2016**, *20*, 243–278. [CrossRef]
28. Bosco, M.; Marino, E.M.; Rossi, P.P. Modelling of steel link beams of short, intermediate or long length. *Eng. Struct.* **2015**, *84*, 406–418. [CrossRef]
29. Bosco, M.; Ghersi, A.; Marino, E.M.; Rossi, P.P. Importance of link models in the assessment of the seismic response of multi-storey EBFs designed by ec8. *Ing. Sismica* **2016**, *33*, 82–93.
30. Bosco, M.; Marino, E.M.; Rossi, P.P. Influence of modelling of steel link beams on the seismic response of EBFs. *Eng. Struct.* **2016**, *127*, 459–474. [CrossRef]
31. Kwon, O.S. *Eqmaker-Artificial Earthquake Maker*; Korea Martial Institute: Kyonggi, Republic of Korea, 2000.
32. *FEMA 356*; Prestandard and Commentary for the Seismic Rehabilitation of Buildings. American Society of Civil Engineers for the Federal Emergency Management Agency: Washington, DC, USA, 2000.
33. Huang, Z.; Cheng, Y.; Zhang, D.; Yan, D.; Shen, Y. Seismic fragility and resilience assessment of shallowly buried large-section underground civil defense structure in soft soils: Framework and application. *Tunn. Undergr. Space Technol.* **2024**, *146*, 105640. [CrossRef]